arXiv:astro-ph/9706199v2 23 Jun 1997

Redshifts of the Gravitational Lenses B1422+231 and PG1115+080[1]

John L. Tonry

Institute for Astronomy, University of Hawaii, Honolulu, HI 96822

Electronic mail: jt@avidya.ifa.hawaii.edu

ABSTRACT

B1422+231 and PG1115+080 are gravitational lens systems producing quadruple QSO images where there is real promise that time delays can constrain the Hubble constant. In addition, the lensing galaxies are both part of groups which can play an important role in modelling the lens potential. This article reports redshifts for the lensing galaxies and three neighboring galaxies in each of the two systems. B1422+231 consists of a group at $z = 0.339$ with a dispersion of $733\,\mathrm{km\,s^{-1}}$, and PG1115+080 is a group at $z = 0.311$ with a dispersion of $326\,\mathrm{km\,s^{-1}}$. One of the neighboring galaxies in the B1422+231 system turned out to be an emission line galaxy at $z = 0.536$, suggesting that QSO light passing through B1422+231 may have been subjected to lensing by a cluster at this more distant redshift. The velocity dispersion of the lensing galaxy in PG1115+080 is determined to be $281 \pm 25\,\mathrm{km\,s^{-1}}$ ($1''$ square aperture), which is surprisingly large given the image splittings of $1.2''$ in that system.

Subject headings: cosmology — distance scale — gravitational lensing — quasars: individual (B1422+231, PG1115+080)

[1]Based on observations at the W. M. Keck Observatory, which is operated jointly by the California Institute of Technology and the University of California

1. Introduction

The differing paths followed by light around a gravitational lens leads to different time of flight. If the lensed source should vary, measurement of a time delay can transform dimensionless redshifts into physical distances, hence provide a Hubble constant (Refsdal 1964). To within factors of order unity the entire time of flight is simply the time delay divided by the square of the image splitting (in radians). In principle this is an extremely powerful method to learn about cosmology; in practice it has proven to be difficult to measure time delays and model lenses accurately enough to challenge the accuracy of 10–20 percent claimed by more traditional measures of H_0. Nevertheless, gravitational lens measurements of cosmology are critically important because they are potentially subject to far fewer biases than the usual distance ladder.

Time delays have now been measured for two lens systems: 0957+561 and PG1115+080. The difficulty in measuring a time delay and then rendering from it cosmological information is illustrated by 0957+561. A time delay was reported by Schild and Cholfin (1986), disputed by Press, Rybicki, and Hewitt (1992), and finally resolved in favor of Schild's number by further observations by Kundić et al. (1996). Models of the system have also undergone improvement, with estimated values for H_0 as low as $50\,\mathrm{km\,s^{-1}\,Mpc^{-1}}$ and as high as $90\,\mathrm{km\,s^{-1}\,Mpc^{-1}}$ (Grogin & Narayan 1996).

PG1115+080 has been observed by Schechter et al. (1997) who derived a time delay and estimated a Hubble constant of $45\,\mathrm{km\,s^{-1}\,Mpc^{-1}}$ based on image and lens positions from Kristian et al. (1993) and a lens redshift of about $z \approx 0.3$ from Henry & Heasley (1986) and Angonin-Willaime et al. (1993). The observations reported here were recently anticipated by Kundić, Cohen, and Blandford (1997, KCB) who find $z = 0.311$, and use this to derive $H_0 = 62 \pm 17$.

B1422+231 is a very well studied QSO and Ly-α system at a redshift of 3.62 discovered by Patnaik et al. (1992), with a lensing galaxy at a redshift of $z = 0.647$ according to Hammer et al. (1995). There is again a small group of three galaxies within a few arcseconds with unknown redshift. Although no time delay has been measured in this system, the photometry compiled by Keeton and Kochanek (1996) suggest that there may be enough variability in the QSO that it should be possible to do so.

This article reports the first results in an ongoing program to measure the most basic information necessary to exploit the gravitational lenses: the redshift of the lensing galaxy, redshifts of galaxies clustered around the lens, and velocity dispersions of the stars within the galaxies. Although a small ingredient compared to measuring time delays and modelling potentials, it is an essential one.

2. Observations and Reductions

B1422+231 and PG1115+080 were observed on March 30 and March 31, 1997 using the Low Resolution Imaging Spectrograph (LRIS) (Oke et al. 1995) at the Keck II telescope on Mauna Kea, along with calibration exposures, an observation of the cluster MS1358+62 to act as a velocity dispersion calibrator, and HD132737 and AGK2+14873 as radial velocity templates. The observations are summarized in Table 1. The sky was clear and the seeing was about $0.8''$ throughout both nights. Long slits of $1.0''$ and $0.7''$ were used

along with gratings of 300 and 600 l/mm, both blazed at 5000Å. The 300 l/mm grating was always rotated to provide coverage from 3800–8700Å, whereas the 600 l/mm grating was rotated either to cover 4800–7680Å for the QSO observations or 3800–6080Å for the templates. The spectral resolution was about 7.9Å FWHM for the 300 l/mm grating, 4.65Å FWHM for the 600 l/mm grating with a 1.0″ slit, 3.59Å FWHM for the 600 l/mm grating with a 0.7″ slit, and the scale along the slit was 0.211″/pixel. The template stars were guided smoothly across the slit in many locations in order to have uniform illumination across the slit, to build up signal to noise, and to map out loci of constant slit position across the detector. The slit was rotated as illustrated in Figure 1, either to observe two companion galaxies simultaneously or else to cover the lensing galaxy while avoiding as much QSO light as possible.

The spectra were reduced using software described in detail by Tonry (1984). The basic steps are to flatten the images, remove cosmic rays, derive a wavelength solution as a function of both row and column using sky lines (wavelengths tabulated by Osterbrock et al. 1996), derive a slit position solution as a function of both row and column using the positions of the template star images in the slit, rebin the entire image to coordinates of log wavelength and slit position, add images, and then sky subtract. A quadratic fit to patches of sky on either side of the object (including a patch between for the galaxy pair observations) did a very good job of removing the sky lines from the spectra.

As has been stressed by Kelson et al. (1997), measuring the velocity dispersion of a galaxy at a redshift significantly larger than zero must be done carefully, since the instrumental

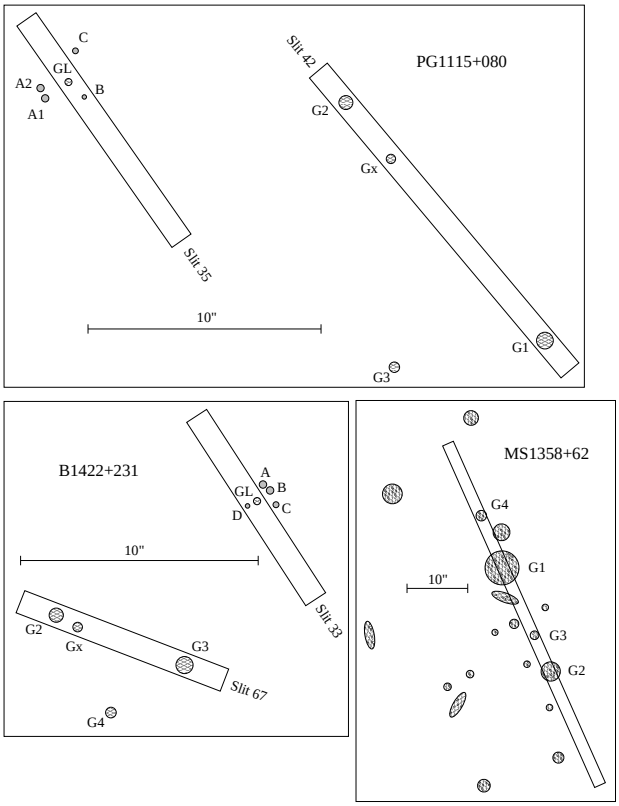

Fig. 1.— Illustration of the slit positions and galaxy idenifications for B1422+231, PG1115+080, and MS1358+62. North is up and East is left for each diagram.

resolution of a spectrograph tends to a constant number of angstroms, whereas the redshifted spectrum has been stretched. Hence a straightforward cross-correlation or Fourier quotient will underestimate the dispersion of the galaxy. Kelson et al. measured dispersions in the cluster MS1358+62 using high resolution template spectra and very careful modelling of the spectrograph resolution derived by measuring sky line widths. The observations here use the trick that the ratio between an $0.7''$ and $1.0''$ slit is slightly larger than $(1+z)$ for these lenses, hence a *template* measured with the $0.7''$ slit will have almost exactly the same instrumental resolution as a *galaxy* at a redshift of $z \approx 0.3$. This is borne out by the ratio of the measured spectral resolutions: $4.65\text{Å} \div 3.59\text{Å} = 1.30$. This is applicable only to the 600 l/mm observations, of course.

As a test that this observing procedure will give correct dispersions, we also observed the cluster MS1358+62 for which Kelson et al. measure a dispersion of 305 ± 5 for the central galaxy, G1, and 213 ± 4 for the neighboring bright galaxy, G2 (Franx, private communication).

The analysis of the companion galaxies was straightforward since the spectra were of very high signal to noise and were uncontaminated by QSO light. In each case the spectrum was extracted, and cross-correlated with the template spectrum according to Tonry and Davis (1979) as well as being analyzed by the Fourier quotient method of Sargent et al. (1977). (The cross-correlation is more robust in the case of low signal to noise, but at the signal levels here the two results are statistically the same, and are simply averaged.) For each spectrum the redshift, error, and velocity dispersion were calculated. The redshift calculation included the entire spectrum, whereas the spectrum blueward of 4000Å (rest frame) was excised for the dispersion calculation, since the calcium H and K lines are so broad that they are always problematic for dispersions. Dispersions are not shown for 300 l/mm observations, and they are not corrected for any aperture effects, hence correspond to an aperture of approximately $1''$ square.

Table 2 lists the redshifts, errors, velocity dispersions, errors, and cross-correlation significance "r" values for each spectrum.

2.1. B1422

We were surprised to find an unmistakable emission line system adjacent to B1422-G2, offset by about $1.0''$ along the line towards B1422-G3. It showed very clear, extended emission lines of 3727 and 5007 in both exposures, and Hβ could also be faintly discerned. Lacking any imaging information on this galaxy, we tabulate it as "B1422-Gx".

The lensing galaxy extractions require considerable care. In the case of B1422 we exploited the fact that the A-B-C components of the QSO would put a more extended distribution of light along the slit than the lensing galaxy. We therefore extracted three swaths of approximately $1''$; the central one we dubbed "QSO+galaxy" and the two flanking swaths we added and dubbed "QSO". Of course there is considerable galaxy light in the flanking swaths but the expectation was that the proportion of galaxy light would be less. We found a linear function of wavelength which, when multiplied by the "QSO" spectrum, would match the Ly-α and C IV QSO lines in the "QSO+galaxy" spectrum. Subtraction left behind a residue which was a clean enough lensing galaxy spectrum that we

could derive a solid cross-correlation redshift.

In principle it would have been better to get a pure QSO spectrum for subtraction, and indeed we obtained a pure QSO spectrum by shifting the slit down on top of the A–C line. However, the QSO light in the composite spectrum has a large gradient across the slit, hence a wavelength shift and large intensity variations. Time did not permit rotating the spectrograph 180 degrees and offsetting to the other side of the QSO to try to duplicate the QSO contribution to the composite spectrum.

We see no emission in the B1422 lensing galaxy whatsoever, despite the claims by Hammer et al. (1995) that 3727 and 5007 appeared at 6138Å and 8247Å. We excised the A and B bands at 7625Å and 6885Å from the spectrum and 130Å centered on the Ly-α peak, and performed a cross-correlation against the template star. The cross-correlation came out with a correlation peak at $z = 0.3366$ with an r value of 4.2, which is significant enough that it is quite unlikely (probability around 1 percent) to be spurious. It is possible to see H+K, Mg, and Na at that redshift. With the corroboration from the neighboring galaxies, we are quite confident that this is indeed the redshift of the lensing galaxy.

The spectra of the QSO, lensing galaxy, G3, G2, and Gx are plotted in Figure 2. The most prominent Fraunhofer lines are labeled for the lensing galaxy, and while they can plausibly be seen by eye, our trust in this redshift ultimately depends on the cross-correlation significance.

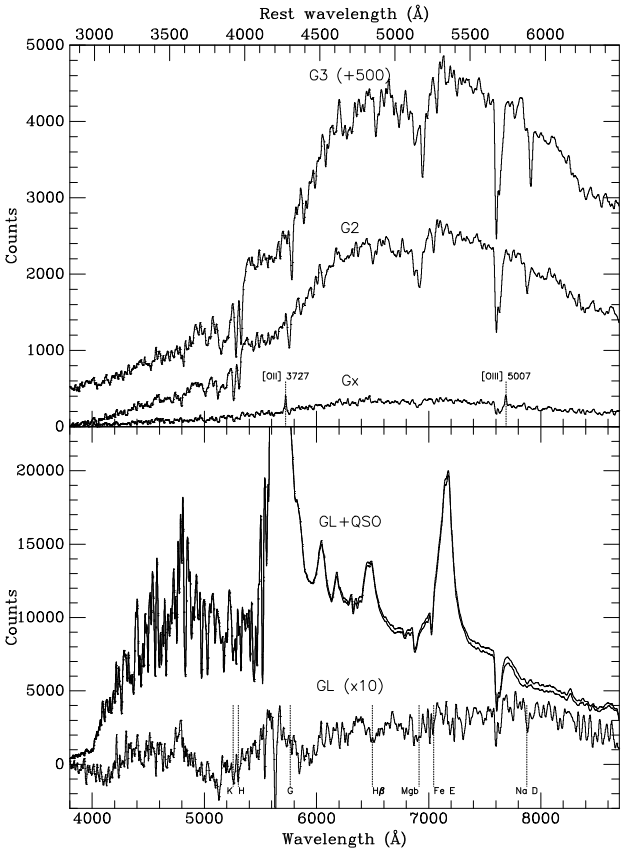

Fig. 2.— The spectra are shown for G3 (offset by 500 for clarity), G2, Gx, QSO+lensing galaxy, "pure" QSO, and extracted lensing galaxy (scaled by a factor of 10 for visibility) in the B1422 system. These spectra have been Gaussian smoothed with a FWHM of 6Å. The top axis shows rest wavelength at a redshift of 0.34. The [OII] and [OIII] lines in Gx are labeled as well as the Fraunhofer lines in GL.

2.2. PG1115

As with B1422, we serendipitously picked up an emission line galaxy in the PG1115 system along the slit between G1 and G2, lying

3.8″ from G2. It displays emission lines of 5007, 4959, H_β, and H_γ, and we refer to it in Table 2 as "PG1115-Gx".

The slit for PG1115 ran over the top of the B QSO component, the lensing galaxy, and skirted the edge of the C component, creating a bimodal distribution of light in the slit with the galaxy in the center. In this case the QSO light illuminated the slit uniformly enough that the subsequent exposure centered on the A1-A2 components matched the QSO light from the B and C to a high degree of accuracy. The B and C peaks were separated by 1.8″ at this position angle, and we extracted the inner 1″ from between the two peaks and subtracted a scaled version of the A1-A2 spectrum to give us the lensing galaxy spectrum illustrated in Figure 3.

Comparison with the redshifts presented by Kundić et al. shows extremely good agreement: GL – 0.3100 KCB, 0.3098 here; G1 – 0.3099 KCB; 0.3098 here; G2 – 0.3120 KCB; 0.3123 here. As noted by KCB, these redshifts are in good agreement with Henry & Heasley (1986), but are only marginally consistent with Angonin-Willaime at al. (1993).

The spectra of the QSO, lensing galaxy, G1, G2, and Gx are plotted in Figure 3.

2.3. MS1358

A pair of exposures of MS1358 identical to those of PG1115 yielded spectra of seven galaxies. The slit was aligned between the central galaxy, called G1 here, and the bright galaxy 19″ to the SW (PA 204), called G2. The galaxies G3 and G4 were well centered in the slit, hence their velocities and dispersions should be reliable. The three remaining galaxies were marginally caught by the slit and low signal-to-noise, so we do not report their velocities. Comparison with Fabricant

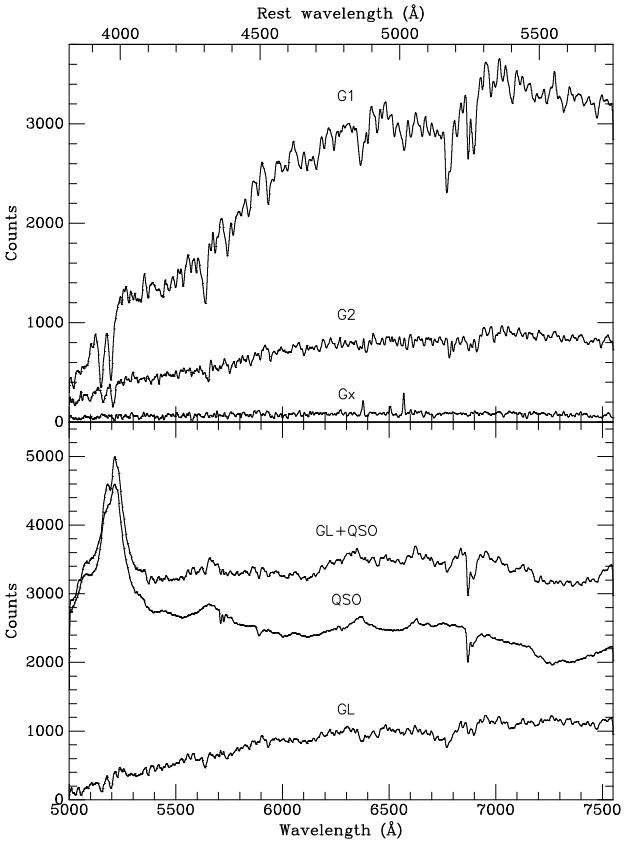

Fig. 3.— The spectra are shown for G1, G2, Gx, QSO+lensing galaxy, pure QSO, and extracted lensing galaxy in the PG1115 system. These spectra have been Gaussian smoothed with a FWHM of 6Å. The top axis shows rest wavelength at a redshift of 0.31. Emission lines of 5007, 4959, and 4861 are apparent in the spectrum of Gx.

et al. (1991) for the three galaxies in common (G1 = #140, G2 = #121, and G3 = #126) gives a mean offset of $\delta z = 0.0002$ and a scatter of $\sigma_z = 0.0001$, well within the error estimates.

The comparison of velocity dispersions with Kelson et al. reveals no significant offset in the dispersions measured here — G1: 305 ± 5 versus 299 ± 22 here; G2: 213 ± 4 versus 235 ± 23 here. The mean of these ratios differs from unity by only 4%, indicating that the dispersions and errors reported here should be accurate.

3. Discussion

Computing means and standard deviations for the redshifts presented here, we find the B1422 lens is part of a group at $z_g = 0.339 \pm 0.002$ with a rest frame dispersion (i.e. standard deviation of cz divided by $1 + z$) of $733\,\mathrm{km\,s^{-1}}$ (3 galaxies). The PG1115 lens is part of a group at $z_g = 0.311 \pm 0.001$ with a rest frame dispersion of $326\,\mathrm{km\,s^{-1}}$ (5 galaxies). Kundić et al. gave $165\,\mathrm{km\,s^{-1}}$ but this is obviously a typographical error which should be $270\,\mathrm{km\,s^{-1}}$, (confirmed by Kundić, private communication). Using the four galaxies observed in the MS1358 cluster we find $z_c = 0.325 \pm 0.001$ with a rest frame dispersion of $432\,\mathrm{km\,s^{-1}}$ (4 galaxies).

A few comments seem appropriate. The B1422 group appears to be quite massive, particularly given the number of galaxies present. Deeper imaging would probably be worthwhile. Despite the comparison Kundić et al. make between the PG1115 and Hickson poor groups (Hickson et al. 1992), it now looks as though the group is much more massive, and the dispersion of $326\,\mathrm{km\,s^{-1}}$ is in quite good agreement with the models of Schechter et al., who need a group dispersion of $383\,\mathrm{km\,s^{-1}}$ to provide the necessary shear to explain the image positions. Finally, the dispersion for MS1358 serves as a warning that small numbers of galaxies near the centers of groups may not be a reliable measure of the overall group mass. Fabricant et al. determine a dispersion of $1125\,\mathrm{km\,s^{-1}}$ for MS1358 from approximately 65 galaxies within 2 arcminutes of the BCG. Recomputing a dispersion from their redshifts but restricting to galaxies closer to the BCG than G2 we find a dispersion of $625\,\mathrm{km\,s^{-1}}$, demonstrating how a cool subsystem can exist in a massive cluster.

The redshift found here for the B1422 system is significantly lower than that reported by Hammer et al., so the lens and companions are not as highly luminous as had been suggested. This lower redshift is in quite good agreement with the redshift estimated photometrically by Impey et al. (1996). The rather high cluster mass called for by Hogg and Blandford (1994) appears to be confirmed here. The presence of the background galaxy at $z = 0.536$ at a distance of $9''$ from the lens may point to a background cluster which is providing significant multiple lensing. Very deep imaging of this source would help elucidate whether there is indeed a background cluster present.

The dispersion for the lensing galaxy in PG1115 of $281\,\mathrm{km\,s^{-1}}$ can be corrected according to the formula given by Jorgensen et al. 1995 to the standard metric aperture commonly used in fundamental plane studies: $3.4''$ at the distance of Coma. This corrected dispersion is $293\,\mathrm{km\,s^{-1}}$ and it seems surprisingly large. Perhaps the best way to see this is to consider the Einstein ring created by an isothermal lens of dispersion σ aligned with the source. This ring will have radius r_0 given

by

$$r_0 = \frac{D_{ds} D_d}{D_s} \frac{4\pi\sigma^2}{c^2}. \quad (1)$$

Using redshifts of $z_s = 1.722$, $z_d = 0.311$, and $\Omega_0 = 1$, we find the first term is $394h^{-1}$ Mpc, and the angular size distance of the lens is $D_d = 580h^{-1}$ Mpc, so that one arcsecond is $2.81h^{-1}$ kpc. This then gives $r_0 = 4.72h^{-1}$ kpc $= 1.68''$. However, the geometric mean of the four QSO positions around the lensing galaxy is $1.17''$, which is the reason that the models of Schechter et al. prefer a dispersion for the lens of about $235\,\mathrm{km\,s^{-1}}$. The position of the ring of images is quite robust to the details of shear and azimuthal image position, so it will take detailed modelling to understand how this high dispersion can fit in with the rest of the observables. It is conceivable that this dispersion is simply wrong, but the spectrum is quite high quality, even given the necessity for QSO subtraction, having a signal to noise of about 20 per angstrom. It is also possible that the dispersion drops rapidly from the measured value of $281\,\mathrm{km\,s^{-1}}$ to something nearer $235\,\mathrm{km\,s^{-1}}$ at the radius of $3.3h^{-1}$ kpc where the images lie. While not unheard of, this would be a surprisingly fast decline in velocity dispersion. While the prospects for spatial resolution in the dispersion are not good, it can be used to constrain possible models for the galaxy: an isothermal mass distribution looks problematic. The models of Keeton and Kochanek (1997) explore some of these possibilities. A final possibility is that the shear from cluster is pushing the images closer together, overcoming some of the splitting from the lens itself, but it is unclear whether such a model could be workable.

In recent years the sophistication of gravitational lens models has clearly outstripped the quality of the data available. The Keck telescopes and the LRIS spectrograph are truly marvelous facilities, and it is the aim of this and subsequent papers to try to bring some grist to the hungry mill, and perhaps help teach us about the cosmology of our universe.

Thanks are due to Paul Schechter for encouragement and helpful suggestions throughout this project.

TABLE 1
OBSERVING LOG.

Obs#	Objects	UT Date	UT	sec z	PA	Exposure	Slit	Grating
1.	AGK2+14783	3/30	5:46	1.01	90		0.7	600/5000
2.	PG1115 GL+B	3/30	8:55	1.02	35	1500	1.0	600/5000
3.	PG1115 GL+B	3/30	9:22	1.02	35	1500	1.0	600/5000
4.	PG1115 A1+A1	3/30	9:53	1.04	35	500	1.0	600/5000
5.	PG1115 G1+G2	3/30	10:10	1.05	42	1500	1.0	600/5000
6.	PG1115 G1+G2	3/30	10:36		42	1500	1.0	600/5000
7.	MS1358 G1+...	3/30	11:12	1.37	24	1500	1.0	600/5000
8.	MS1358 G1+...	3/30	11:39	1.36	24	1500	1.0	600/5000
9.	B1422 G2+G3	3/30	12:21	1.00	67	1500	1.0	300/5000
10.	B1422 G2+G3	3/30	12:47		67	1500	1.0	300/5000
11.	B1422 GL	3/30	13:54	1.09	33	1500	1.0	300/5000
12.	B1422 GL	3/30	14:21	1.15	33	1500	1.0	300/5000
13.	HD132737	3/30	15:11	1.20	90		1.0	300/5000
14.	HD132737	3/30	15:23		90		0.7	600/5000
15.	AGK2+14783	3/31	5:26	1.01	90		0.7	600/5000
16.	AGK2+14783	3/31	5:45	1.01	90		1.0	300/5000
17.	PG1115 GL+B	3/31	8:11	1.04	35	1500	0.7	300/5000
18.	PG1115 GL+B	3/31	8:35	1.02	35	1500	0.7	300/5000
19.	PG1115 A1+A2	3/31	9:05	1.02	35	500	1.0	300/5000

NOTE.—PA is east from north, exposures are in seconds, slit widths are in arcseconds.

TABLE 2
REDSHIFTS AND DISPERSIONS.

Galaxy	y	z	$\pm$	σ	$\pm$	r
B1422-GL		0.3366	0.0004			4.2
B1422-G2	-2.9	0.3376	0.0001			13.0
B1422-G3	$+2.9$	0.3427	0.0001			11.4
B1422-Gx	-1.9	0.5360	0.0005			em.
PG1115-GL		0.3098	0.0002	281	25	10.4
PG1115-G1	-6.7	0.3098	0.0001	256	20	14.8
PG1115-G2	$+6.7$	0.3123	0.0001	130	60	10.9
PG1115-Gx	$+2.9$	0.3121	0.0002			em.
PG1115-GL		0.3095	0.0002			8.1
MS1358-G1	$+9.6$	0.3272	0.0001	299	22	11.9
MS1358-G2	-9.5	0.3235	0.0001	235	23	14.1
MS1358-G3	-1.7	0.3248	0.0001	155	56	9.4
MS1358-G4	$+18.3$	0.3229	0.0002	175	86	5.2

NOTE.—Columns: Galaxy name, slit position ($''$), redshift and error, velocity dispersion ($\mathrm{km\,s^{-1}}$) and error, cross-correlation r value.

REFERENCES

Angonin-Willaime, M.-C., Hammer, F., & Rigaut, F. 1993, in Gravitational Lenses in the Unverse, eds. J. Surdej, D. Fraipont-Caro, E. Gosset, S. Refsdal, & M. Remy (Liège: Institute d'Astrophysique), 85

Fabricant, D.G., McClintock, J.E. & Bautz, M.W. 1991, ApJ, 381, 33.

Grogin, N.A. & Narayan, R 1996 ApJ, 464, 92, and 473, 570.

Hammer, F., Rigaut, F., Angonin-Willaime, M.-C., Vanderriest, C. 1995, A&A, 298, 737.

Henry, J.P., & Heasley, J.N. 1986, Nature, 321, 139.

Hickson, P., Mendes de Oliveira, C., Huchra, J.P., & Palumbo, G.G.C. 1992, ApJ, 399, 353.

Hogg, D.W., & Blandford, R.D. 1994, MNRAS, 268, 889.

Impey, C.D., Foltz, C.B., Petry, C.E., Browne, I.W.A., & Patnaik, A.R. 1996, ApJ, 462, L53.

Jorgensen, I., Franx, M., & Kjaergaard, P. 1995, MNRAS, 276, 1341.

Keeton, C.R., & Kochanek, C.S. 1997, preprint.

Keeton, C.R., & Kochanek, C.S. 1996, in Astrophysical Applications of Gravitational Lensing, eds. C.S. Kochanek & J.N. Hewitt (IAU: Netherlands), 419.

Kelson, D.D., van Dokkum, P.G., Franx, M., Illingworth, G.D. & Fabricant, D. 1997, *eprint* astro-ph 9701115v2.

Kristian, J., Groth, E.J., Shaya, E.J., Schneider, D.P. & Holtzman, J.A. 1993, AJ, 106, 1330

Kundić, T., Colley, W.N., Gott, J.R., Malhotra, S., Pen, U., Rhoads, J.E., Stanek, K.Z., & Turner, E.L. 1995, ApJ, 455, L5.

Kundić, T., Cohen, J.G., & Blandford, R.D. 1997, *eprint* astro-ph 9704109 (KCB).

Oke, J.B., et al. 1995, PASP, 107, 375.

Osterbrock, D.E., Fulbright, J.P., Martel, A.R., Keane, M.J., & Trager, S.C. 1996, PASP, 108, 277

Patnaik, A.R., Browne, I.W.A., Walsh, D., Chaffee, F.H., & Foltz, C.B. 1992, MNRAS, 259, 1p.

Press, W.H., Rybicki, G.B., & Hewitt, J.N. 1992, ApJ, 385, 404.

Refsdal, S. 1964 MNRAS, 128, 307.

Sargent, W.L.W., Schechter, P.L., Boksenberg, A., & Shortridge, K. 1977, ApJ, 212, 326.

Schechter, P.L. et al. 1997, ApJ, 475, L85.

Schild, R.E., & Cholfin, B. 1986, ApJ, 300, 209.

Tonry, J.L. 1984, ApJ, 279, 13.

Tonry, J.L. & Davis, M. 1979, AJ, 84, 1511.

This 2-column preprint was prepared with the AAS LaTeX macros v4.0.